Kurdish Studies
Feb 2024
Volume: 12, No: 2, pp.1468-1479
ISSN: 2051-4883 (Print) | ISSN 2051-4891 (Online)
www.KurdishStudies.net

Received: December 2023 Accepted: January 2024
DOI: https://doi.org/10.58262/ks.v12i2.109

Statistical Analysis of the Technical Condition of the Irrigation Pipeline of the Community of San José De La Silveria through the Measurement of Thicknesses by Ultrasound

Calderón Freire Edisson Fernando[1], Redroban Dillon Cristian David[2], Andino Célleri Lourdes Valeria[3], Vistin Vistin Jair Manuel[4]

Abstract

Wear caused by the presence of solid particles. It is essential to precisely identify the specific causes of wear caused by the presence of solid particles, because it has a negative influence on both water quality and the efficiency of the distribution system, which generates significant costs. To carry out this research, the pulse-echo ultrasonic method is used, according to ASTM E797 standard, for which the TG3000 ultrasonic equipment is used and the guidelines established by API 570 standard for the inspection and evaluation of thicknesses are followed. It is important to note that the intrinsic properties of the materials, such as propagation, microstructure dispersion and attenuation, pose challenges in the application of ultrasound as a measurement technique. Thickness measurements are carried out on 15 pipe sections, using reference points (TML) as a tool for identification. Pipe wear is determined at measurement points along a 15,000-meter inspection length. The measurement of the points along the pipeline is established at a distance between points of 1 m with respect to the total length. Then, digital statistical tools, such as R-study, are used to analyze the most prone areas that require immediate maintenance. Finally, it is concluded that the wear originating inside the pipe is due to hydro-abrasion. These findings offer valuable insight into wear mechanisms, providing a solid basis for the implementation of preventive strategies and effective maintenance, thus contributing to the preservation of the integrity and efficiency of the water pipeline system.

Keywords: *wear; pipeline; ultrasonic; hydro-abrasion; ASTM E797; pulse-echo; erosion; corrosion; abrasion; abrasion.*

1. Introduction

Erosion-corrosion is the primary cause of premature failure of various flow management components; such as pipes, pumps, valves, impellers, hydro-turbines, etc. In many industries, this phenomenon occurs due to the well-known interaction between mechanical erosion and corrosion resulting from the relative motion between a corrosive fluid and a material surface. Especially for pipeline, which is the key component in the transportation of fluids containing liquids (such as oil and water) and solid particles (such as sand), it has been documented that

[1] Escuela Politécnica Nacional, Facultad de Ingeniería Mecánica, Quito, Ecuador, Email: edisson.calderon@epn.edu.ec
Orcid: https://orcid.org/0000-0002-3955-8162
[2] Escuela Superior Politécnica de Chimborazo, Facultad de Mecánica, Carrera de Ingeniería Automotriz Riobamba, Ecuador
Email: david.redroban@espoch.edu.ec, Orcid: https://orcid.org/0000-0003-3543-9390
[3] Escuela Superior Politécnica de Chimborazo, Riobamba, Ecuador, Email: valeria.andino@espoch.edu.ec, Orcid: 0009-0009-6350-9633
[4] Universidad Estatal de Bolívar, Facultad de Ciencias de la Educación, Sociales, Filosóficas y Humanísticas Carrera Pedagogía de las Ciencias Experimentales- Informática, Guaranda, Ecuador, Email: jvistin@ueb.edu.ec, Orcid: https://orcid.org/0000-0002-7434-0329

erosion and corrosion damage can cost the global transmission pipeline industry billions of dollars annually, in addition to irreversible damage to life and the environment. In addition, corrosion damage is typically contributed by four parts: pure corrosion, pure erosion, erosion-enhanced corrosion, and corrosion-enhanced erosion (Wood, 2006)(Revie, 2011)(Wood, 2006)

Therefore, the transition from the erosion-corrosion mechanism of the dominated mixture to the erosion-dissolution/passivation of the dominant damage generally corresponds to the transition of the degree of damage from mild to severe. (al., 2010)

According to the results of the gas pipeline safety assessment conducted by Student et al. (2018), stress corrosion cracking is the leading cause of pipeline accidents. Cracks are mainly caused by corrosion pitting on the outer surface of the pipe in areas where the protective cover is damaged, while the pipe is subject to prolonged combined action of operating stresses caused by the internal pressure of the gas. (API., 1998)

The study of the morphology and structure of the oxide layer complements the understanding of the properties of corrosion products, because the more compact and dense they are, the greater the corrosion protection layer obtained [5,6]. In the initial stages of oxide layer formation, lepidocrocite (γ-FeOOH) is formed, which is subsequently transformed into goethite (α-FeOOH), which is the thermodynamically stable phase. After that, the corrosion rate of the steel is greatly reduced (API., 1998)(Carreño, 2017)

The non-destructive control (NDT) technique is one of the best methods of defect evaluation which allows to identify the structural damage of the first stage, in order to prevent structural failures and reduce economic losses. One of the advantages of this technique is the remote control, which reduces operating costs, downtime, etc. . (Carreño, 2017) (Cenicaña., 2015.)(Chimeneas, 2020.)(Corporation, 2019.)

Ultrasonic waves have established themselves as a non-destructive testing technology. In some nations, such as Japan, the ultrasound research method has been standardized as a test method for compressive strength and as an estimate of the depth of cracks in materials.

Pipelines are a crucial means of transporting oil and gas. In these, cracks can be seen in the pipes, which cause accidents due to leaks and considerable losses. Therefore, the initial detection of cracks must be timely and effective. Currently, the magnetic flux leakage inspection method and the ultrasonic inspection method are commonly used to test pipes. Ultrasonic inspection technology has developed rapidly in recent years, because it is highly efficient and detects more types of defects than other methods. (A53/A53M-99:, 1999) (Alcaraz, 2016)(API., 1998)(Applus., 2019.)

Most of the existing industrial tools that are placed inside pipes for ultrasonic inspection adopt acoustic beams that propagate with normal incidence. This step is suitable for inspecting defects caused by changes in pipe wall thickness. However, these methods are insensitive to cracks, particularly those with small dimensions. In light of this shortcoming, numerous ultrasonic inspection tools have been developed to improve inspection performance, including the establishment of composite ultrasound or the transducer array space model.

2. Methodology

The irrigation water pipe that is analyzed for thickness measurement starts from the community of Urbina to the community of Cuatro Esquinas. For the thickness intake, the 7545 km long

pipeline is divided into 15 sections, where 14 of these sections are 500 m long and one is 545 m long. The division of the sections of the irrigation pipeline and their trajectory are represented in the following figures:

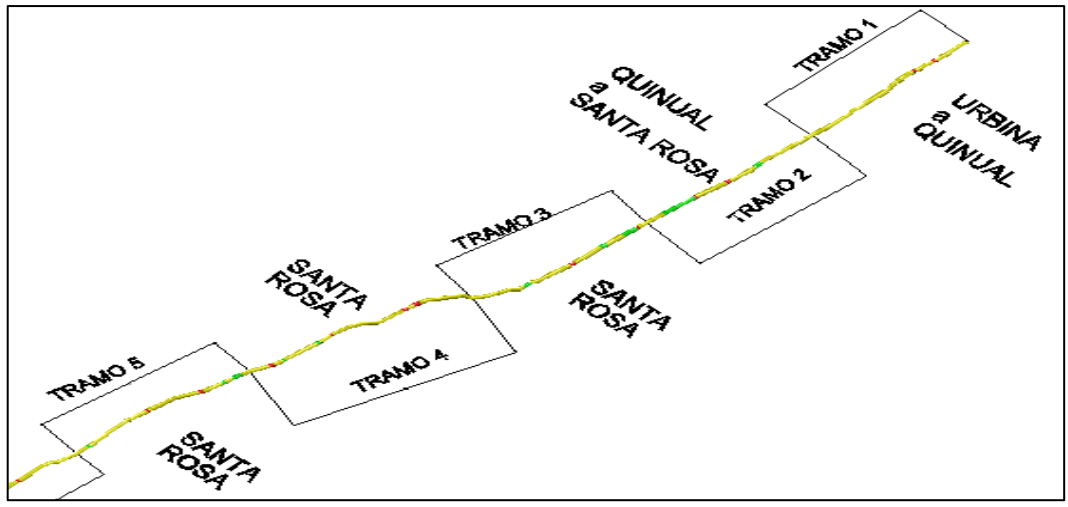

Fig: 1

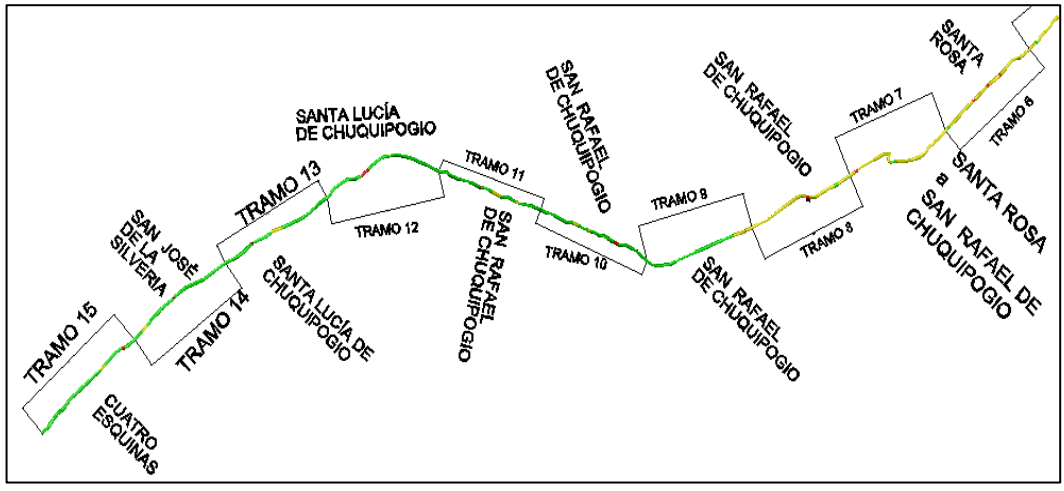

Fig: 2

ASTM E797 provides guidelines for measuring wall thickness using the pulse-echo contact method through ultrasound for materials where their ultrasonic waves propagate at a constant rate throughout their structure at temperatures not exceeding 93°C.

The API 570 standard is used to determine the service life, wear rate, and frequencies of upcoming inspections on the pipeline being analyzed.

To calculate the wear rate, the following equation is used in section 7.1.1 of this standard (Data Inspection, Analysis and Evaluation).

$$V_{desgaste} = \frac{t_{inicial} - t_{real}}{\Delta t}$$

3. Data Obtained and Calculated

Based on the median and standard deviation, a normality test is applied, which helps to contrast the hypothesis that "p-value is greater than 0.005"; and with the help of the statistical software R, a statistical analysis of each section of pipe is carried out, where the following box and mustache diagrams of each section are obtained:

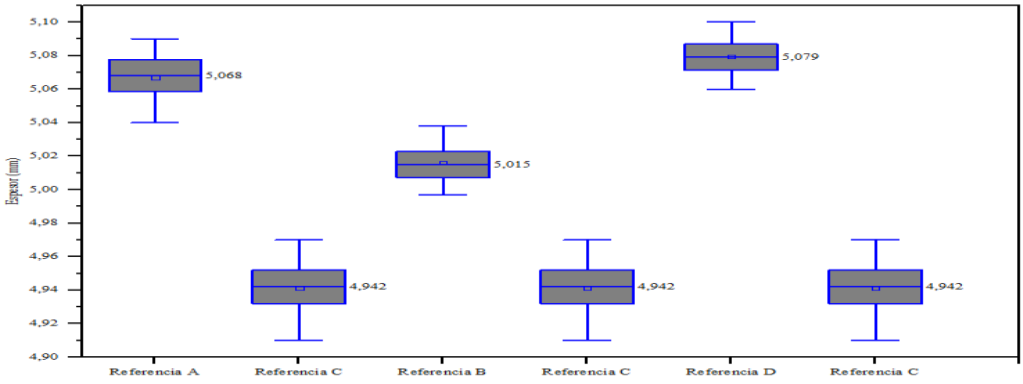

Fig. 3: Box and Mustache Diagram of Section No. 1. Fountain.

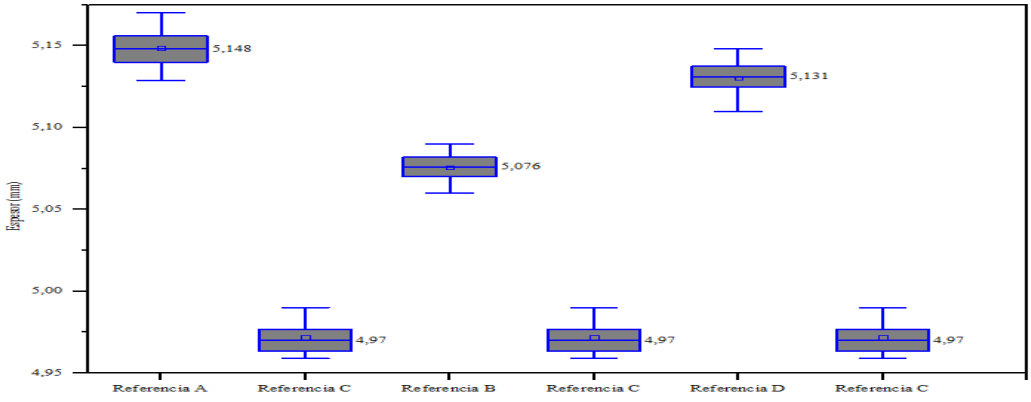

Fig. 4: Box and Mustache Diagram of Section No. 2. Fountain.

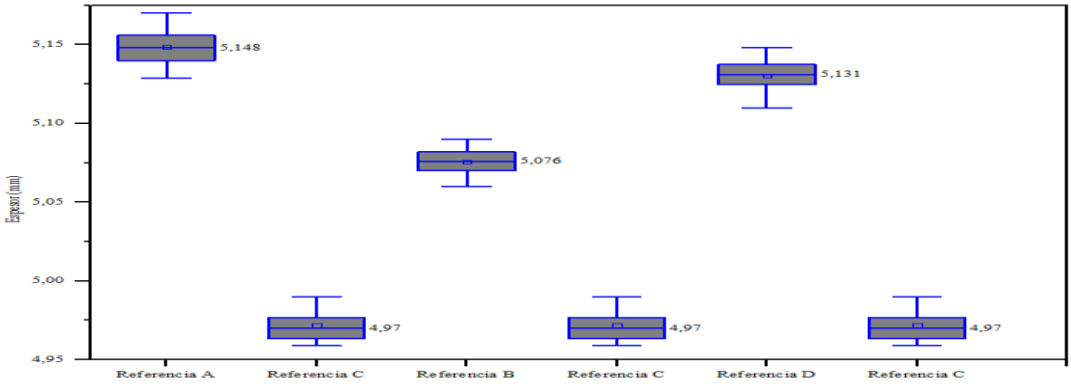

Fig. 5: Box and Mustache Diagram of Section No. 3. Fountain.

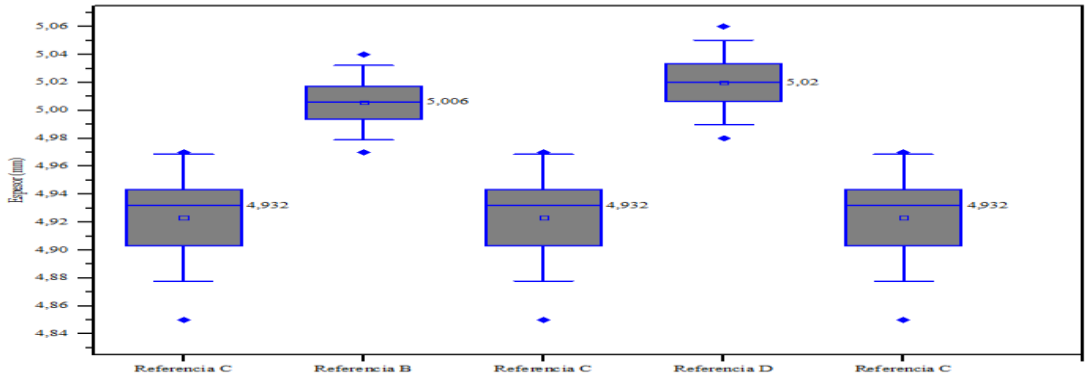

Fig. 6: Box and Mustache Diagram of Section No. 7. Fountain:

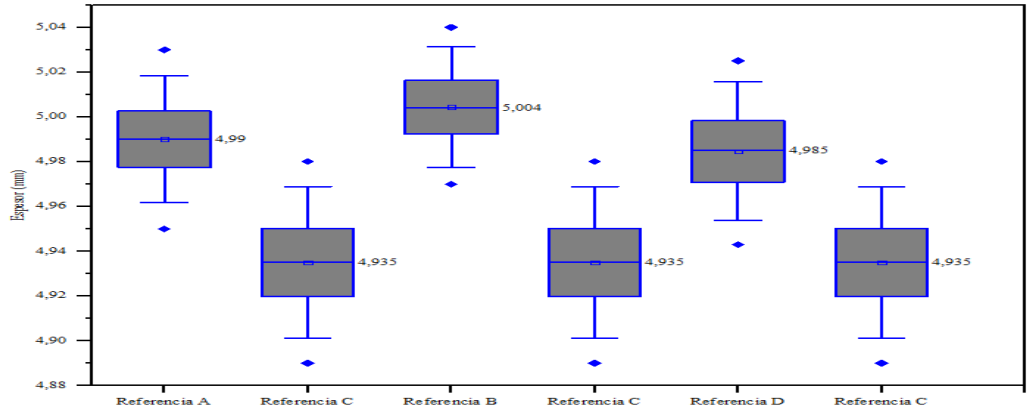

Fig. 7: Box and Mustache Diagram of Section No. 8. Fountain.

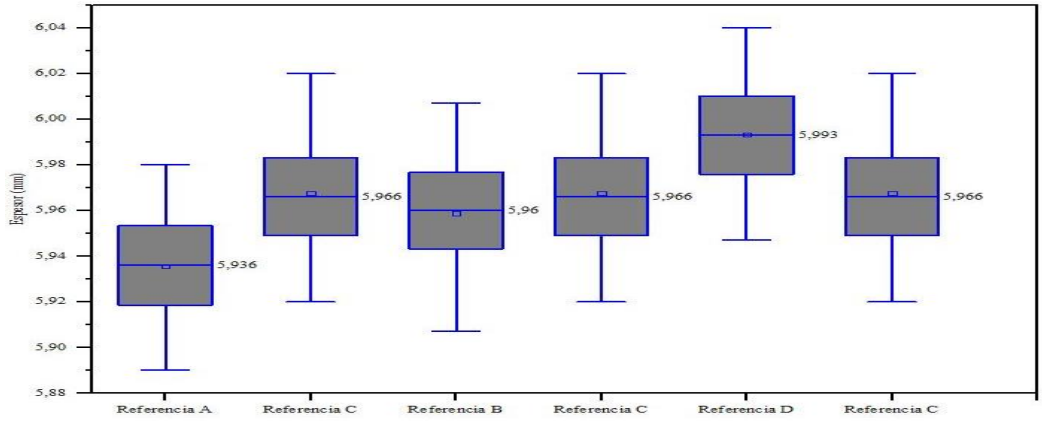

Fig. 8: Box and Mustache Diagram of Section No. 15. Fountain.

It is considered that the data obtained from the 15 sections and at the two weld points with their respective references are a function of the normality test where it is established that the hypothesis raised is greater than 0.05. Thus, in order to comply with the normal distribution, the following tables are obtained for the respective comparative analysis of the sections with greater and lesser thickness.

Board 1 Summary of Greater Thickness as a Function of the Median.

Sections	Distance [m]	Sample [n]	Benchmark	Medium Thickness [mm]
1	0-500	501	D	5,079
2	501-1,000	499	To	5,148
3	1,001-1,500	500	D	5,079
4	1,501-2,000	500	D	5.065
5	2,001-2,500	500	D	5,066
6	2,501-3,000	500	B	4,972
7	3,001-3,500	500	D	5,020
8	3,501-4,000	500	B	5,004
9	4,001-4,500	500	B	5,505
10	4,501-5,000	500	D	5,896
11	5,001-5,500	500	D	5,936
12	5,501-6,000	500	D	6,012
13	6,001-6,500	500	D	6,006
14	6,501-7,000	500	D	5,965
15	7,000-7,548	548	D	5,993
PAS	0-7,548	652	D	5,508
PDS	0-7,548	680	D	5,496

Based on the data set out in the **Error! Reference source not found.**, The medians of each section are represented in the Fig. 9 for their respective thickness analysis, where it is observed that section 12 has a greater thickness trend at reference point D, while section 6 presents a lower thickness within reference point B.

Based on the nominal thickness value of 7.11 mm, proposed by Quinchuela in 2021, an average wear of 1.66 mm is observed at reference points A, B and D, which represent a minimum wear of 25.4% due to the location of these reference points, as can be seen in Fig. 2 resulting in less fluid alteration and a lower wear rate.

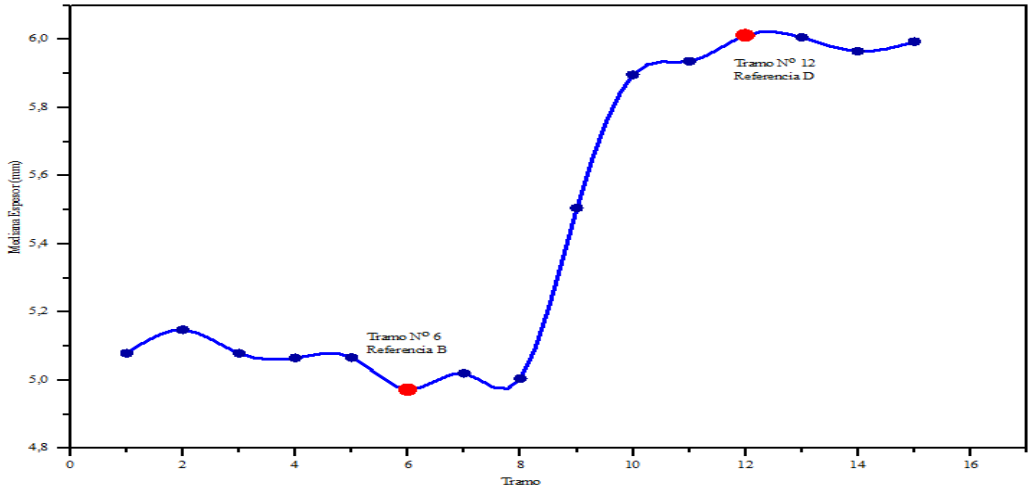

Fig. 9: Trend Curve Thicker than the Median. Fountain.

As for the analysis of the smallest thickness as a function of the mean, with the data presented in the Board 2, The Fig. 10, where it can be observed that section 15 has a greater thickness, while in section 6 there is a lower trend in terms of lower thickness. It is important to note that reference point C, within the 15 sections, is more random.

Based on the nominal thickness of 7.11 mm, an average wear of 1.76 mm is generated within the reference point C, which presents greater wear with a material loss of 74.6% progressively, due to the fact that the reference point is located at the top of the pipe, where there is a greater alteration of fluid and a higher wear velocity. This is due to the particles contained in the irrigation water.

Board 2 Summary of Lower Thickness Depending on the Median.

Sections	Distance [m]	Sample [n]	Benchmark	Medium Thickness [mm]
1	0-500	501	C	4,942
2	501-1,000	499	C	4,970
3	1,001-1,500	500	C	4,915
4	1,501-2,000	500	C	5,000
5	2,001-2,500	500	C	5,001
6	2,501-3,000	500	C	4,885
7	3,001-3,500	500	C	4,932
8	3,501-4,000	500	C	4,935
9	4,001-4,500	500	C	5,402
10	4,501-5,000	500	C	5,789
11	5,001-5,500	500	C	5,787
12	5,501-6,000	500	C	5,914
13	6,001-6,500	500	C	5,919
14	6,501-7,000	500	C	5,884
15	7,000-7,548	548	To	5,936
PAS	0-7,548	652	C	5,378
PDS	0-7,548	680	C	5,393

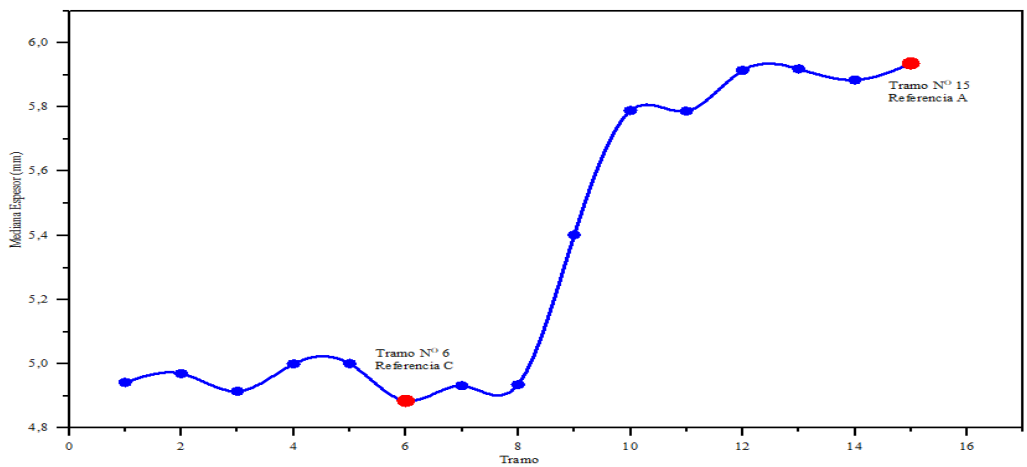

Fig. 10: Trend Curve of Lower Thickness than the Median. Fountain.

Regarding the dispersion of data obtained for each section, the following is obtained: Board 3, with a summary of the largest standard deviation of each benchmark per section.

Board 3 Summary of the Largest Deviation.

Sections	Distance [m]	Sample [n]	Benchmark	Standard deviation [mm]
1	0-500	501	C	0,0101
2	501-1,000	499	To	0,0081
3	1,001-1,500	500	To	0,0085
4	1,501-2,000	500	C	0,0161
5	2,001-2,500	500	C	0,0177
6	2,501-3,000	500	C	0,0180
7	3,001-3,500	500	To	0,0156
8	3,501-4,000	500	C	0,0163
9	4,001-4,500	500	D	0,0265
10	4,501-5,000	500	C	0,0190
11	5,001-5,500	500	To	0,0202
12	5,501-6,000	500	To	0,0179
13	6,001-6,500	500	B	0,0174
14	6,501-7,000	500	B	0,0192
15	7,000-7,548	548	To	0,0174
PAS	0-7,548	652	B	0,0231
PDS	0-7,548	680	C	0,0216

On the basis of the data presented in the Board 3herself points out that reference point D in section 9 has a greater dispersion of data, since the data are heterogeneous due to the gradual loss of surface material at that reference point, in the Fig. 11herself Look at the dispersion of data by each leg. As can be seen in the Fig. 11, Reference point A of section 2 has a lower dispersion of data, due to the homogeneous data, which is caused by sediments and particles present at the top of the pipe.

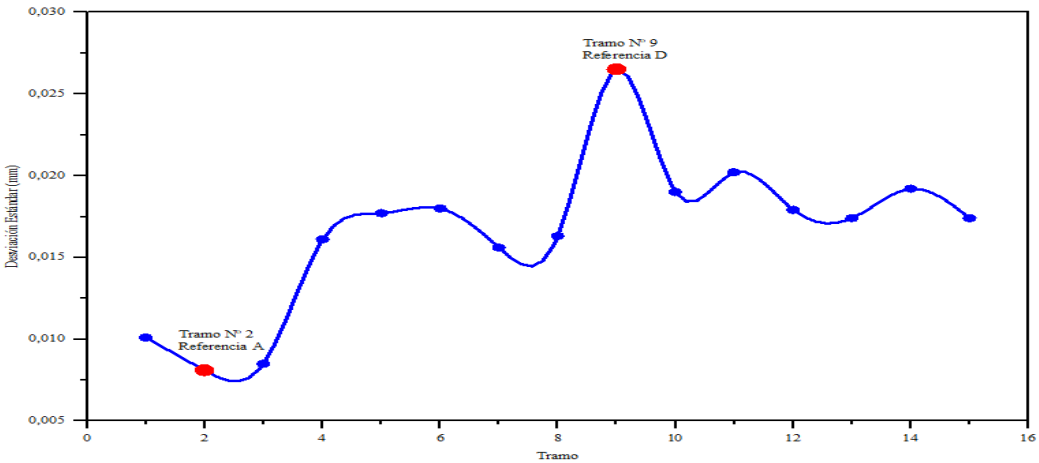

Fig. 11: Trend Curve with the Highest Standard Deviation. Fountain.

3. Analysis of Results

In addition to the data presented above, the Board 4; where it is observed that the results show that the greatest thickness is at the reference point D, which implies that in these sections there is less fluid alteration and lower wear speed.

Regarding the highest standard deviation, it is evident that the reference point D presents heterogeneous data, therefore, the wear most frequently is of the minimal abrasive type, which is caused by the loss of the material over time.

In terms of lower thickness and standard deviation, the C reference point has greater randomness within 15 sections, resulting in abrasive wear, which is caused by scratches, cuts, and chipping that, in the long run, minimize the useful life of the pipe.

Finally, for section 6, the average wear is 4.94 mm, which presents a progressive loss of material within reference points B, C and D, caused by the flow alteration.

Board 4 Results Obtained Through Thickness Analysis.

Function Type	Benchmark	Wear	Cause
Increased thickness	Reference D	Abrasion	Gradual loss of material
Thinner thickness	Reference C	Abrasion	Particulate pollutants from irrigation water
Higher standard deviation	Reference D	Abrasion	Gradual loss of material
Lower standard deviation	Reference B	Abrasion	Particulate pollutants from irrigation water
Section N° 6	Reference B Reference C	Abrasion	Accumulation of particles, due to being in a low and high area

The maximum service life of the sections of the irrigation pipeline is 18 years and their corrosion rate is 0.0716 mm/year. The minimum service life is 15 years and the corrosion rate is in the range of 0.051 mm/year. A correlation analysis confirms that the higher the corrosion rate, the shorter the service life. The opposite occurs when the wear rate is lower, i.e. the lower the corrosion rate, the longer the service life.

Board 5

PUNTOS	(A) 0°	(B) 90°	(C) 180°	(D) 270°	MEDICIÓN MAS BAJA	MEDICIÓN MAS ALTA	OBSERVACIONES
0	5,3	5,1	5,3	5,3	5,1	5,3	
1	5,1	4,7	4,7	5	4,7	5,1	
2	5	5,2	4,9	5,1	4,9	5,2	
3	5,2	5,1	5	5,3	5	5,3	
4	5,3	5,2	5,1	5,2	5,1	5,3	
5	5,4	5,2	4,9	5,3	4,9	5,4	
6	4,8	5,1	4,8	5,2	4,8	5,2	
PAS	4,8	4,5	4,6	5	4,5	5	Punto antes de la soldadura
PDS	5,2	4,7	4,3	4,9	4,3	5,2	Punto después de la soldadura
7	4,9	5	4,6	5	4,6	5	
8	5,2	5,2	5,1	5,3	5,1	5,3	
9	5,1	5,1	5	5,4	5	5,4	
10	5,4	5,1	4,9	5,1	4,9	5,4	

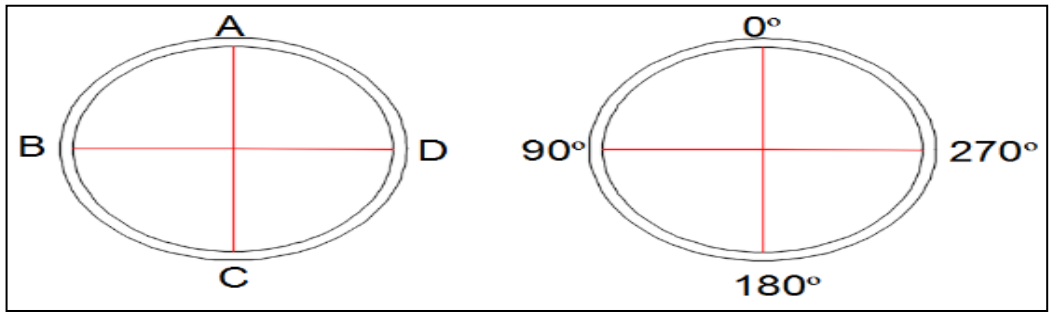

Fig. 12

4. Conclusions

- With the application of pulse-echo ultrasound for irrigation water systems, which are divided into 15 sections with their respective reference points A, B, C and D, it serves as an important instrument for the prediction of wear and the respective analysis of the factors that contribute to it, being in our case the polluting particles of the irrigation water, The gradual loss of material over the years is the main cause of internal wear of pipes due to abrasion.
- This work exposes the great potential presented by ultrasonic measurement using the pulse-echo technique, in the measurement of the thickness of pipes without requiring a stop during the measurement, based on norms and standardizations of procedures, however, there is still the challenge presented by materials, during ultrasonic measurement, since each material has different characteristics such as attenuation and wave speed.
- The types of corrosion that occur in the black steel irrigation water pipe in the community of San José de la Silveria are galvanic and induced, due to the fact that the natural water that circulates along the irrigation pipe is aggressive against this type of steel. These types of corrosion depend on some factors such as the concentration of dissolved oxygen, hydrogen potential (pH), temperature or the concentration of chlorides and sulfates. The aforementioned factors have a direct impact on a reduction in pipe thickness.
- The study highlights the importance of understanding the factors that contribute to wear, focusing on thickness analysis by pulse-echo ultrasound. Accurate thickness measurement in water pipes is identified as a critical task to ensure the structural integrity and safety of these systems. On the other hand, ultrasound emerges as an effective technique that allows these measurements to be made without interrupting the flow of the fluid or making significant modifications to the pipe.
- The influence of various environmental factors, such as salinity, pH, temperature, humidity and the presence of chlorides, affects the wear of steel used in pipes. It is highlighted that pitting corrosion can arise under specific conditions, weakening affected areas and reducing load-bearing capacity. In addition, the relationship between corrosion resistance and factors such as temperature, chloride concentrations and moisture content in concrete is noted.

5. References

1. A53/A53M, ASTM. 1999. Standard Specification for Pipes, Steel, Black & Hot-Dipped & Zinc-Coated, Welded & Seamless. 1999.
2. Water, National Commission of the. 2017. Handbook of Drinking Water, Sewerage and Sanitation. Manual of Drinking Water, Sewerage and Healing. [Online] 2017. [Cited on: 22 January 2020.] http://aneas.com.mx/wp-content/uploads/2016/04/SGAPDS-1-15-Libro10.pdf.
3. Alamy. 2008. Balinese terraced rice fields, governed by a subak (irrigation system) in the Tegallalang area, Bali, Indonesia. [Online] 23 February 2008. [Cited on: 2020 January 24.] https://www.alamy.es/foto-campos-de-arroz-en-terrazas-balinesa-regida-por-un-subak-sistema-de-riego-en-el-area-de-tegallalang-bali-indonesia-171421600.html.
4. Alcaraz, Raúl Bragado. 2016. Corrosion and Enclosure in Irrigation Systems . [Online] Tiloom, October 21, 2016. [Cited on: 29 January 2020.] https://www.tiloom.com/corrosion-e-incrustaciones-en-sistemas-de-riego/.

5. API. 1998. Pipeline Inspection Code. 1998. 570.
6. Applus. 2019. Manual thickness measurement by ultrasound. [Online] Applus Ecuador, 2019. [Cited on: 2020 January 24.] https://www.applus.com/ec/es/what-we-do/sub-service-sheet/medici%C3%B3n-manual-de-espesores-por-ultrasonidos.
7. ASTM. 2001. Standard Practice for Thickness Measurement Using the Manual Pulse-Echo Ultrasound Method. 2001. E797.
8. Bauer, Horts. 1996. Handbook of Automotive Technology. Barcelona : Editorial Reverte, S.A, 1996. ISBN: 84-291-4806-X.
9. Carmona, Rafael Pérez. 2013. Design and construction of sewers. Bogotá : Ecoe Ediciones, 2013. ISBN: 978-958-771-028-1.
10. Carreño, Juan López. 2017. Installation assembly techniques. Madrid : Ediciones Paraninfo, 2017. ISBN: 978-84-283-9652-3.
11. Cenicaña. 2015. Furrow irrigation. [Online] April 6, 2015. [Cited on: 2020 January 24.] https://www.cenicana.org/riego-por-surcos/.
12. Chimneys, Rock. 2020. VITRIF black steel tube. [Online] 2020. [Cited on: 2020 January 24.] https://chimeneasroca.com/49-tubo-acero-negro-vitrif.
13. Corporation, Huatec Group. 2019. TG3000 Ultrasonic Thickness Gauge. Instruction manual. [Online] 2019. [Cited on: 29 January 2020.] www.huatecgroup.com. H00319052006.
14. Curacreto. 2014. CURAFERRO PMX RP-05. [Online] CURACRETO S.A. DE C.V., 2014. [Cited on: 2020-02-26.] https://www.curacreto.com.mx/recubrimientos/industriales/curaferro-pmx-rp-05.html.
15. Dinocorsa. 2017. Five factors that cause corrosion in steel pipes. [Online] Dinocorsa, May 31, 2017. [Cited on: 27 February 2020.] https://www.dincorsa.com/blog/factores-generan-corrosion-tuberias-acero/.
16. Ecured. 2011. Furrow irrigation. [Online] 2011. [Cited on: 2020 January 24.] https://www.ecured.cu/Riego_por_surcos.
17. ELAPLAS. Physical properties of polyvinyl chloride. Rigid PVC. [Online] [Cited on: 2020 January 22.] http://www.elaplas.es/wp-content/uploads/pvc_rigido.pdf.
18. Epoxy, Resin. 2019. What is epoxy resin? [Online] Epoxy resin, 2019. [Cited on: 26 February 2020.] https://laresinaepoxi.com/resina-epoxica/.
19. Falesa. 2015. Irrigation system. How to make a home sprinkler irrigation system. [Online] 2015. [Cited on: 23 January 2020.] https://sistemasderiego.net/sistema-de-riego-casero-por-aspersion/.
20. GADPRSA. 2015. Development and land use plan for the parish of San Andrés. Plan for the development and land use of the parish of San Andrés. Guano : GADPRSA, October 30, 2015.
21. Genescá, Joan. 1995. Corrosion induced by water contamination. [Online] FONDO DE CULTURA ECONÓMICA, 1995. [Cited on: 29 January 2020.] http://bibliotecadigital.ilce.edu.mx/sites/ciencia/volumen3/ciencia3/121/htm/sec_7.htm. ISBN: 968-16-4370-4.
22. Gonzalez, Magdalena. 2017. Sheets and Steels. Differences and Uses of Black and Galvanized Steel Pipe. [Online] Sheets and Steels, May 29, 2017. [Cited on: 2020 January 24.] https://blog.laminasyaceros.com/blog/tuber%C3%ADa-de-acero.
23. Guzmán, Richad. 2002. Irrigation systems. La Paz : Between the lines. Communication, 2002. 99905-68--01-4.
24. Huatec. 2011. Professional testing equipment. Ultrasonic flaw detector. [Online] HUATEC GROUP CORPORATION, 2011. [Cited on: 2020 January 24.] http://spanish.huatecgroup.com/sale-8849-transducer-models-ultrasonic-thickness-gauge-tg3000-for-metals-plastic-ceramics.html.

25. Installations, Assembly Techniques. Galvanized steel pipes. Properties of galvanized steel pipes [Online] [Cited on: 2020 January 22.] http://www.imacifp.com/wp-content/uploads/2013/09/C.F.G.M.-tuber%C3%ADas.pdf.
26. Intertek. 2018. Conventional Ultrasonic Testing. Impulse-Echo Technique. Non-Destructive Testing by Conventional Ultrasound
27. by the Impulse-Echo technique. [Online] Intertek Total Quality Assured, 2018. [Cited on: 2020 January 24.] https://www.intertek.es/ensayos-no-destructivos/ultrasonidos/tecnica-pulso-eco/.